Interfacial Energetics of Protein Adsorption from Aqueous Buffer to Surfaces with Varying Hydrophilicity

A Contribution from the Hematology at Biomaterial Interfaces Research Group

By

Paul Cha,[†] Anandi Krishnan,[‡] Vincent F. Fiore,[‡] and Erwin A. Vogler[*†‡§]

Departments of Materials Science and Engineering[†] and Bioengineering,[‡]
Materials Research Institute and Huck Institute of Life Sciences[§]
The Pennsylvania State University
University Park, PA 16802

* Author to whom correspondence should be addressed **EAV3@PSU.EDU**

Key words: Protein Adsorption, solid-water interface, blood proteins SAM, self-assembled monolayer, Gibbs' Excess

Running title: Interfacial Energetics of Protein Adsorption

Abstract:

Adsorption isotherms constructed from concentration-dependent advancing contact angles θ_a show that the profound biochemical diversity among ten different blood proteins with molecular weight spanning 10-1000 kDa has little discernable effect on the amount adsorbed from aqueous phosphate-buffer saline (PBS) solution to a particular test surface selected from the full range of observable water wettability (as quantified by PBS adhesion tension $\tau_a^o = \gamma_{lv}^o \cos\theta_a^o$; where γ_{lv}^o is the liquid-vapor interfacial tension and θ_a^o is the advancing PBS contact angle). The maximum advancing spreading pressure, $\Pi_a^{\max}$, determined from adsorption isotherms decreases systematically with τ_a^o for methyl-terminated self-assembled monolayers (CH_3 SAM, τ^o =-15 mN/m), polystyrene spun-coated onto electronic-grade SiO_x wafers (PS, τ^o =7.2 mN/m), aminopropyltriethoxysilane-treated SiO_x surfaces (APTES, τ^o =42 mN/m), and fully-water wettable SiO_x (τ^o =72 mN/m). Likewise, the apparent Gibbs' surface excess $\left[\Gamma_{sl} - \Gamma_{sv}\right]$, which measures the difference in the amount of protein adsorbed Γ (moles/cm^2) at solid-vapor (SV) and solid-liquid (SL) interfaces, decreases with τ^o from maximal values measured on the CH_3 SAM surface through zero (no protein adsorption) near $\tau^o = 30$ mN/m ($\theta_a = 65^o$). These latter results corroborate the conclusion drawn from independent studies that water is too strongly bound to surfaces with $\tau^o \geq 30$ mN/m to be displaced by adsorbing protein and that, as a consequence, protein does not accumulate within the interfacial region of such surfaces at concentrations exceeding that of bulk solution ($\left[\Gamma_{sl} - \Gamma_{sv}\right] = 0$ at $\tau^o = 30$ mN/m). Results are collectively interpreted to mean that water controls protein adsorption to surfaces and that the mechanism of protein adsorption can be understood from this perspective for a diverse set of proteins with very different amino-acid composition.

1. Introduction

Many water-soluble biological macromolecules such as proteins are amphiphilic in nature and exhibit the surface-active property of adsorption to interfaces. These so-called "biosurfactant" properties[1] ultimately originate in the differential interactions of water with amphiphilic portions or domains on the solvent-exposed surface of the macromolecule.[2] Biosurfactant adsorption is technically important because it mediates fouling. Fouling is a collection of phenomena by which working surfaces of devices, instruments, or machines in contact with natural aqueous solutions become coated with a layer or layers of adventitious contamination that compromises intended performance. Fouling has broad technologic importance with considerable socioeconomic impact spanning environment, medicine, and transportation (*e.g.* occlusion of pipes and filters used in civil engineering, reduction in biosensor sensitivity, and resistance to the flow of water across boat hulls, respectively). As a consequence, protein adsorption continues to be a phenomenon of great practical importance and is of fundamental interest in surface science.

A full appreciation of the basic mechanisms underlying protein adsorption from aqueous solution requires a complete mass and energy "inventory" that accounts for the distribution of both solvent (water) and solute (protein) molecules between interfacial and solution regions, as well as the energy expended in moving these molecules from one region to another. Toward resolving such an inventory for blood proteins of biomedical interest, we have extensively applied tensiometry (contact angle and wetting methods)[3-12] and the solution-depletion method.[13-16] In particular, we have used time-and-concentration-dependent tensiometry to measure interfacial energetics of protein adsorption to hydrophobic surfaces[3-9] and interpreted these results in terms of amount adsorbed using standard Gibbsian surface thermodynamics.[10, 11] The depletion method, implemented with gel electrophoresis as a separation and quantification tool, allowed us to quantify protein partition coefficients that measure adsorption

affinity for different surfaces,[13, 14] as well as study adsorption competition among a mixture of proteins for the same adsorbent surface.[15]

This paper reports use of time-and-concentration-dependent tensiometry to measure interfacial energetics of protein adsorption to surfaces spanning the full observable range of water wettability. Results confirm that Gibbsian surface thermodynamics can be used to model interfacial energetics deduced from advancing contact angles under experimental conditions that avoid uncontrolled protein deposition at the solid-vapor (SV) interface. We further show that variation in the molecular structure of different proteins has little discernable effect on the interfacial energetics that drives protein adsorption from aqueous solution.

2. Methods and Materials

Purified Proteins and Synthetic Surfactants: Table 1 compiles pertinent details on proteins used in this work. Protein purity was certified by the vendor to be no less than the respective values listed in Column 4 of Table 1, as ascertained by electrophoresis (SDS-PAGE or IEP). Mass, concentration, and molecular weights supplied with purified proteins were accepted without further confirmation. Issues associated with protein purity, especially contamination with surfactants, and the potential effect on measured interfacial tensions have been discussed elsewhere.[3] The single value given in Table 1 (Column 5) for physiological concentration of human proteins applied in this work was middle of the range listed by Putnam[17] or Anderson.[18] Serial dilutions of stock protein solutions (usually 10 mg/mL) were performed in 96-well microtiter plates by (typically) 50:50 dilution in phosphate buffered saline solution (PBS; 0.14 M NaCl, 0.003M KCl) prepared from powder (Sigma Aldrich) in distilled-deionized (18.2 MΩ-cm) water using procedures detailed in ref. 3. Between 24-30 dilutions were prepared in this manner, covering a dynamic range between 10^{-10} % to 1% (w/v), taking care to mix each dilution by repeated pipette aspiration and avoiding foaming of concentrated solutions.

Test Surfaces: Data for methyl-terminated self-assembled monolayer surfaces (CH_3 SAM) was taken from ref. 7 and preparation procedures are disclosed therein. Briefly, p-type <111> electronic grade silicon wafers (Montco Silicon Technologies, Inc., Spring City, PA) were pre-cleaned in hot 1:4 H_2O_2 (30%)/H_2SO_4 followed by rinsing with distilled-deionized H_2O and absolute ethanol.[19-25] Gold-coated wafers were prepared by vapor deposition of chromium and gold (99.99% purity) from resistively-heated tungsten boats onto clean 3-in. diameter silicon wafers at about 1 x 10^{-8} torr base pressure in a cryogenically pumped deposition chamber. The sample was not allowed to rise above ~40^{o}C during the evaporation. Film thicknesses, monitored with a quartz crystal oscillator, were typically 15 nm and 200 nm for chromium and gold, respectively. Chromium was deposited prior to gold to enhance adhesion to the substrate.

After deposition, the chamber was backfilled with research-grade nitrogen. Gold-coated samples were removed and immersed in 1mM solutions of 1-hexadecanethiol ($CH_3(CH_2)_{15}SH$) in ethanol, contained in glass jars at ambient temperature, for at least 3 days. The alkanethiol (Aldrich Chemical Co., Milwaukee, WI) and ethanol (commercial reagent-grade) were used as-received, without further purification. Samples were stored in the thiol solution until use and were rinsed with ethanol just prior to an experiment.

Polystyrene (PS) and aminopropyltriethoxysilane-treated (APTES) surfaces were prepared by spin-coating or silanization, respectively. Silicon wafers prepared as above were further oxidized by 12 min. air plasma treatment (producing a surface referred to as SiO_x). A thin PS layer was applied by spin coating 1 mL of PS dissolved in reagent-grade toluene solution for 120 s at 5000 rpm in a spin-coating unit (Brewer Science, Inc., Rolla, MO). PS solution was made by dissolving bacteriological grade PS culture dishes (Corning, Inc., Corning, NY) to a concentration of 80 mg/mL. Conformal coatings were confirmed by visual inspection supplemented with "breath figures".[26-28] Profilometry (KLA-Tencor Corp., San José, CA) further confirmed surface quality and demonstrated <10 nm root mean square (RMS) roughness. Atomic Force Microscopy (AFM) indicated a 0.24 nm RMS roughness consistent with literature reports.[29] APTES surfaces were prepared by immersing SiO_x surfaces (as above) in 10% APTES solution in absolute ethanol for 30 min. followed by 24 hr cure at 110°C in a vacuum oven. APTES, ethanol, chloroform, and toluene were used as-received from the vendor (Aldrich Chemical Co., Milwaukee, WI). Surfaces were used in tensiometric experiments directly after preparation.

Tensiometry & Goniometry: Liquid-vapor (LV) interfacial tensions of protein solutions required by this work were measured by Pendant Drop Tensiometry (PDT) as described in refs. 3, 4. Tilting-Plate Goniometry (TPG) was performed using a commercial automated goniometer

(First Ten Angstroms Inc., Portsmouth, VA). The tilting-plate goniometer employed a Tecan liquid-handling robot to aspirate 12 μL of protein solutions contained in a 96-well microtiter plate prepared by the serial-dilution protocol mentioned above. The robot was used to reproducibly transfer the tip with fluid contents into a humidified (99+ % RH) analysis chamber and dispense 10 μL drops of protein solution onto the surface of test substrata (see below) held within the focal plane of a magnifying camera. These and all other aspects of TPG were performed under computer control. Proprietary algorithms supplied by the vendor were used to deduce contact angles from drop images captured at a programmed rate by a frame grabber. Typically, 600 images were captured at a rate of 1 image every 6 sec following 20 sec delay to permit vibrations of the expelled drop to dampen. Drop evaporation rates within the humidified chamber deduced from computed-drop volumes (based on image analysis) were observed to vary with solute concentration, generally ranging from approximately 25 nL/min for pure water to 10 nL/min for solute solutions > 0.1% w/v. The impact of this evaporation rate over the 60 min time frame of the experiment was apparently negligible, as gauged from the behavior of purified surfactants reported elsewhere.[4, 7] Precision of θ_a was about $\pm 0.5^o$ based on repeated measurement of the same drop. The analysis chamber was thermostated to a lower-limit of 25 ± 1 ^{o}C by means of a computer-controlled resistive heater. Upper-temperature limit was not controlled but rather floated with laboratory temperature, which occasionally drifted as high as 29 ^{o}C during summer months. Thus, reported θ_a values were probably not more accurate than about 1^o on an inter-sample basis considering the small, but measurable, variation of water interfacial tension with temperature. This range of accuracy was deemed adequate to the conclusions of this report which do not strongly depend on highly accurate θ_a that is difficult to achieve on a routine basis. Instead, veracity of arguments raised herein depend more on a breadth of reliable measurements made across the general family of human proteins.

Test substrata were held on a rotating, tilting-plate platform driven by stepper motors under computer control. Substrata were allowed to come to equilibrium within the sample-chamber environment for no less than 30 min before contact angle measurements were initiated. The platform was programmed to tilt at 1°/sec from horizontal to 25° after the drop was deposited on the surface by the robot. The optimal (incipient rolling) tilt angle was found to be 25° and 15° for solutions of proteins and surfactants respectively. The first 20 images monitored evolution of the advancing angle. At the end of the 1 hr θ_a measurement period, the platform was programmed to return to horizontal and rotate 15° to the next analysis position along the periphery of the semiconductor wafer. This process was repeated for all dilutions of the protein under study so that results reported for each protein were obtained on a single test surface, eliminating the possibility of substratum-to-substratum variation within reported results.

θ_a measurements by TPG employed in this work were verified against Wilhelmy-balance tensiometry (WBT) and found to agree within a percentage difference of 2.5±1.9% for $50^\circ < \theta_a < 120^\circ$.[30] Receding angles ($\theta_r$) were shown to be not as reliable as θ_a and, as a consequence, only θ_a was analyzed in this work. It is worthwhile mentioning in this context that WBT itself is inappropriate for studies of protein adsorption at the SL interface (at least as applied herein) because (i) the technique requires thin plates that are difficult to two-side coat with gold for thiol-SAM preparation, (ii) WBT generally requires high solution volumes (~ 10 mL) that greatly exceed availability of purified proteins, and (iii) the moving three-phase line deposits solute (protein) at the SV interface making interpretation of the Gibbs' surface excess parameter $\left[\Gamma_{sl} - \Gamma_{sv}\right]$ highly ambiguous.[1] Overall, we have found the tilting-plate method applicable to measuring adsorption, at least for hydrophobic and modestly hydrophilic surfaces $\theta_a > 50^\circ$, and suitable for 1 hr equilibration times if a humidified chamber is used to control evaporation.[10, 11]

However, it was observed that surfaces studied herein were slightly unstable and subject to "hydration" that led to a systematic decrease in water/PBS contact angles with time. These hydration dynamics were observed to be more pronounced on test surfaces that had been incubated for long periods (> 3 d) in the 100% RH atmosphere of the PDT analysis chamber (not shown). However, we do not believe this slight but apparently unavoidable attribute of surfaces supported on silicon wafers negatively affects the veracity of conclusions based on final, steady-state Π_a measurements made at ~ 1 hr analysis time (see further below).

Theoretical Interpretation of Data: Adsorption of proteins was observed to affect liquid-vapor (LV) interfacial tensions and produced concentration-dependent change in measured contact angles θ, suggesting that either or both solid-vapor (SV) and solid-liquid (SL) tensions were likewise affected by protein adsorption. Contact angles were quantified using the Young equation $\tau \equiv \gamma_{lv}\cos\theta = \gamma_{sv} - \gamma_{sl}$; where τ is adhesion tension and γ the tension at the interface denoted by subscripts. Thus, contact angles were used to monitor adsorption to solid surfaces in accordance with refs. 1, 10, 11 and citations therein. Contact-angle isotherms monitored effects of adsorption by plotting advancing contact angles θ_a against $\ln C_B$ (see Fig. 1 for examples); where bulk-phase concentrations C_B range from 10^{-10} to 1 % (w/v, see Materials and Methods). Contact-angle isotherms were sequentially interpreted in terms of adhesion-tension (τ_a vs. $\ln C_B$) and spreading-pressure (Π_a vs. $\ln C_B$) isotherms; where $\tau_a \equiv \gamma_{lv}\cos\theta_a$, $\Pi_a = \left(\tau_a - \tau_a^o\right)$, γ_{lv} is the LV interfacial tension of the fluid at C_B, and τ_a^o is the adhesion tension of pure PBS buffer ($\gamma_{lv}^o = 71.97\text{mN/m at } 20^\circ\text{C}$). We monitored time dependence of all three isotherm forms but herein interpreted only final measurements that achieve or approach steady-state (a pseudo or "meso" equilibrium).[31] Issues associated with steady-state adsorption and reversibility are taken up in the Discussion section.

Secure interpretation of measured θ_a in terms of τ_a depended on accurate knowledge of γ_{lv} at the bulk-phase surfactant concentration in equilibrium with SL and LV interfaces. Thus, depletion of the bulk phase by solute adsorption might require, in some circumstances, correction of as-prepared bulk-solution concentration C_B. However, we have demonstrated statistical agreement between (uncorrected) tensiometry results and independent instrumental methods of measuring adsorption for surfactants, showing that solute-depletion was not a serious issue for surfactant standards under experimental conditions of this work.[7] Likewise, for the specific case of protein adsorption, it has been concluded from a simple calculation that solute depletion was not a serious problem requiring correction because the absolute amount of protein adsorbed from solution was, at most, only of the order of 0.2% for a hydrophobic surface at surface-saturating protein concentrations.[8]

Practical use of concentration-dependent contact angles as a measure of adsorption to the SL interface has been discussed at length elsewhere (see, for examples, refs. 1, 10, 11 and citations therein). Briefly, for the purposes of this paper, the amount of solute adsorbed to SV and SL interfaces was measured by the Gibbs' surface excess quantities Γ_{sv} and Γ_{sl}, respectively, in units of moles/area (the subscript "a" specifying advancing contact angles is not carried in Γ symbology for the sake of notational compactness). The difference $\left[\Gamma_{\mathrm{sl}} - \Gamma_{sv}\right]$ (but not separate excess parameters) was computed from data comprising contact-angle isotherms using Eq. (1):

$$\left[\Gamma_{\mathrm{sl}} - \Gamma_{sv}\right] = -\left\{\frac{\left[\gamma_{lv}\sin\theta_a\right]}{RT}\left(\frac{d\theta_a}{d\ln C_B}\right) + \left[\Gamma_{lv}\cos\theta_a\right]\right\} \qquad (1)$$

where $d\theta_a / d\ln C_B$ is the slope of a contact-angle isotherm. $\Gamma_{lv} = -\frac{1}{RT}\left(\frac{d\gamma_{lv}}{d\ln C_B}\right)$ is the surface excess at the LV interface determined from separate measurement of concentration-dependent γ_{lv} of the solute under study.[4] This form of the Gibbs' adsorption isotherm was appropriate for a single, isomerically-pure non-ionizing solute or a polyelectrolyte in swamping salt concentrations of buffer salts.[4, 32] It is also important to stress that $\left[\Gamma_{\mathrm{sl}} - \Gamma_{sv}\right]$ and Γ_{lv} values obtained without correcting concentration C_B for solute activity were "apparent" surface excess values that can substantially deviate from the authentic surface excess calculated from $\left(d\theta_a / d\mu\right)$ and $\left(d\gamma_{lv}/d\mu\right)$; where μ is activity-corrected chemical potential.[4, 33, 34] However, previous work suggests that the discrepancy between apparent and actual Γ_{lv} is roughly constant for the proteins of this study and apparent surface excess was about 60X larger than actual surface excess,[4, 7] presumably because of the substantial non-ideality of complex polyelectrolytes. We thus assumed in this work that apparent $\left[\Gamma_{\mathrm{sl}} - \Gamma_{sv}\right]$ was also 60X larger than the actual, activity-corrected surface excess because the ratio $\left\{\frac{\left[\Gamma_{\mathrm{sl}} - \Gamma_{sv}\right]}{\Gamma_{lv}}\right\}$~1 for hydrophobic surfaces for which Γ_{sv} ~ 0 (as discussed further below). Comparison of tensiometric and instrumental measures of adsorption of surfactant standards confirms this factor.[7]

For surfaces exhibiting θ_a > 60° and under experimental conditions that avoid inadvertent mechanical deposition of solute at the (SV) interface, as through drop movement on the surface or evaporation for examples, it has been shown that Γ_{sv} ~ 0 and $\left[\Gamma_{\mathrm{sl}} - \Gamma_{sv}\right] \rightarrow \Gamma_{\mathrm{sl}}$.[1, 10, 11] Under the additional restrictions that (i) solute activities at SL and LV interfaces are approximately

equal and (ii) $\Gamma_{sl} \sim \Gamma_{lv}$, it can be expected that $\left\{\frac{\left[\Gamma_{sl}-\Gamma_{sv}\right]}{\Gamma_{lv}}\right\} \sim 1$. Experimental results confirm that these stringent physical conditions prevail for LV and CH_3 SAM surfaces and it is therefore concluded that apparent $\left[\Gamma_{sl}-\Gamma_{sv}\right] \sim \Gamma_{sl}$ for proteins reported herein adsorbing to hydrophobic surfaces.[7] However, solute adsorption to the SV interface becomes increasingly pronounced with increasing hydrophilicity which caused $\left[\Gamma_{sl}-\Gamma_{sv}\right] < 0$, as further described in refs. 10, 11.

Computation and Data Representation: Computational, statistical, and theoretical methods used in this work have been discussed in detail elsewhere.[1, 3, 4, 8, 10, 11] Briefly, time-dependent θ_a data corresponding to protein dilutions (see above) were recovered from TPG files and correlated with concentrations, leading to a matrix of results with row values representing concentration and time (in sec) as column values. It was generally observed that θ_a isotherms were sigmoidal in shape when plotted on logarithmic-concentration axes,[1, 10] with well-defined low-concentration asymptote θ_a^o and high-concentration asymptote $\theta_a^{'}$ (see Fig. 1). Successive non-linear least-squares fitting of a four-parameter logistic equation $\left[\theta_a = \frac{\theta_a^{\circ} - \theta_a^{'}}{1+(\ln C_B^{\Theta/2} / \ln C_B)^M} + \theta_a^{'}\right]$ to contact angle isotherms data for each time within the observation interval quantified parameters θ_a^o and $\theta_a^{'}$ with a measure of statistical uncertainty.[1, 10, 11] Fitting also recovered a parameter measuring concentration-at-half-maximal-change in θ_a, $\ln C_B^{\Theta/2}$ (where $\Theta/2 = 1/2\Theta^{\max}$ and $\Theta^{\max} \equiv \theta_a^{\circ} - \theta_a^{'}$), as well as a parameter M that measured steepness of the sigmoidal curve. This multi-parameter fitting to concentration-dependent θ_a data was a purely pragmatic strategy that permitted quantification of best-fit protein and surfactant characteristics but is not a theory-based analysis.[1, 3, 4, 6, 10, 11] Three-dimensional (3D)

representations of time-and-concentration-dependent θ_a data were created in Sigma Plot (v9) from the data matrix discussed above and overlain onto fitted-mesh computed from least-squares fitting. Two-dimensional (2D) representations were created from the same data matrices at selected observation times. Measured θ_a were converted to advancing adhesion tension $\tau_a = \gamma_{lv} \cos\theta_a$ for general interpretation;[1] where γ_{lv} was the interfacial tension of the contact-angle fluid. Adhesion tensions $\tau_a^o = \gamma_{lv}^o \cos\theta_a^o$ (pure saline) and $\tau_a^{'} = \gamma_{lv}^{'} \cos\theta_a^{'}$ (at the minimum contact angle observed $\theta_a^{'}$) were computed with fitted parameters γ_{lv}° and $\gamma_{lv}^{'}$ reported in refs. 3, 4 for the proteins under investigation. Smoothed adhesion-tension isotherms (τ_a vs. $\ln C_B$) were computed from smoothed θ_a using smoothed γ_{lv} values computed from best-fit parameters reported in refs. 3, 4. Likewise, smoothed spreading pressure isotherms (Π_a vs. $\ln C_B$) were computed from smoothed τ_a curves, where $\Pi_a \equiv \left(\tau_a - \tau_a^{\circ}\right)$.

4.0 Results

Surface Stability: Pure PBS advancing contact angles θ_a^o on spun-coated polystyrene (PS) and aminopropyltriethoxysilane-treated (APTES) SiO_x surfaces were observed to monotonically decrease with observation time while PBS interfacial tension γ_{lv} (measured by PDT) remained constant, as shown in Fig. 2 (compare open and closed circles). Specifically, it was observed that θ_a^o of a pure PBS droplet on PS slowly decreased with time from the initial value of 91º< θ_a^o <89º at t = 0 to 86º< θ_a^o <84º at t = 1 h. The range of reported results corresponds to all 10 PS surfaces analyzed during the course of this work. A similar effect was noticed on all 4 APTES surfaces analyzed during the course of this work, although a wider range among all 4 APTES surfaces at t=0 was observed. A similar phenomenon was observed in the methyl-terminated SAM case.[7] Constant γ_{lv} is strong evidence that the PBS used in contact angle

measurements was not contaminated with surface active solute(s) that adsorb to surfaces. We are thus inclined to attribute this modest decrease in test-surface wettability with time to "surface hydration" in which water slowly permeates into the near surface region, increasing wettability of test surfaces.[7] Surface hydration apparently affected time-dependent measurement of protein-solution contact angles because we observed that the whole contact angle isotherm (θ_a vs. concentration) slowly shifted lower with time (see Fig. 1, annotation in Panel B). Steady-state spreading pressure Π_a isotherms effectively correct for the SAM hydration effect in the adsorption measurement by normalizing to final τ_a^o; that is to say time-dependent, $\Pi_a = \left(\tau_a - \tau_a^o\right)$ subtracts any time dependence in τ_a^o. A similar strategy was applied to analysis of protein adsorption kinetics, as further illustrated in Fig. 2 (compare closed triangles and open triangles). At any time t, reduction in pure PBS contact angle due to hydration (closed circles, Fig. 2) was added to the recorded θ_a for a protein-containing solution (closed triangles) to 'correct' observed θ_a for the hydration effect (open triangles). This correction procedure typically eliminated the long-term downward drift in θ_a observed for protein-containing solutions (see filled triangles, Fig. 2 for example), suggesting that protein-adsorption kinetics had, in fact, dampened within the 1 hr observation period; as had been generally observed for adsorption of these same proteins at the LV surface[3-6, 35] for which no such hydration phenomena occurs.

General Aspects of Adsorption Data: Fig. 1 compares contact-angle isotherms obtained for the proteolytic enzyme thrombin (blood factor IIa, FIIa) adsorbing to methyl-terminated SAM (previously reported in ref. 7), PS, and APTES surfaces. Isotherms for all proteins listed in Table 1 were similar and apparently reached or asymptotically approached steady state when data was corrected for surface hydration as discussed above. The full-range effect on θ_a at steady state was less than about 20°, especially for APTES for which a definitive affect by

adsorption was difficult to discern (Panel C, Fig. 1). Table 2 compiles quantitative parameters derived from statistical fitting of data that permits numerical comparison of adsorption results to CH_3 SAM, PS, and APTES surfaces. Contact angle parameters θ_a^o, $\theta_a^{'}$, $\ln C_B^{\Theta/2}$ and M listed in cols 2-5 of Table 2 are the mean fitted values corresponding to final 25 θ_a curves recorded within the 60-minute time frame of the TPG experiment. Listed error is standard deviation of this mean. Ubiquitin does not saturate the interface, as previously observed for the CH_3 SAM surface. Table 2 lists only graphical estimates of parameters (see ref. 7 for more discussion).

Fig. 3 traces sequential interpretation of steady-state (1 hr drop age), concentration-dependent θ_a data (Panel A) in terms of concentration-dependent adhesion tension τ_a (Panel B) and spreading pressure Π_a (Panel C) for human serum albumin (FV HSA). Steady-state (equilibrium) spreading pressure isotherms Π_a were used as the basis of comparison of protein adsorption for the compounds listed in Table 1. Corresponding adhesion tensions τ_a° and $\tau_a^{'}$ (Table 2, columns 6, 7) were computed from θ_a^o and $\theta_a^{'}$ values, respectively, with uncertainty estimates computed by propagation of error in θ_a and γ_{lv} measurements (Materials and Methods). Maximum spreading pressure $\Pi_a^{\max} \equiv \left(\tau_a^{'} - \tau_a^{\circ}\right)$ (Column 8) was computed directly from aforementioned τ_a values and associated uncertainty again estimated by propagation of error. No data is listed in Table 2 for water-wettable SiO_x surfaces because both PBS and protein solutions spread with contact angle less than 10^o, implying that no protein adsorbed to water wettable surfaces, in corroboration of previous studies.[10-12, 14] Otherwise, if protein adsorbed to water-wetted SiO_x surfaces, contact angles would be expected to rise as a result of the accumulation of relatively hydrophobic organic matter. Indeed, trace contamination of hydrophilic surfaces is very easy to detect and can be troublesome to avoid.[36]

Fig. 4 collects Π_a isotherms for selected proteins spanning the molecular weight range 10 < MW < 1000 kDa adsorbing to the PS surface. Only smoothed curves are shown for the sake of clarity, but representative θ_a, τ_a, and Π_a isotherms with authentic data are amply illustrated in Figs. 1, 3. The dynamic range of Π_a ~ 20 mN/m was similar to that observed for these proteins at the buffer-air[3, 4] and CH_3 SAM surface[8, 9] and $\Pi_a^{\max}$ fell within a relatively narrow 5 mN/m band for the diverse set of proteins studied.[4] Furthermore, the 'Traube-rule-like' ordering of protein adsorption observed at the LV interface[4] was repeated at the SL interface in that high-MW proteins reduce Π_a to any arbitrary value at lower molarity than low-MW proteins, as suggested by the horizontal arrow annotation on Fig. 4.

Apparent Gibbs' Surface Excess: Adsorption to the solid-liquid (SL) surface was interpreted in terms of the apparent Gibbs' excess parameter $\left[\Gamma_{\mathrm{sl}} - \Gamma_{sv}\right]$ computed using Eq. (1) applied to contact-angle isotherms (see ref. 7 for example calculations). As noted previously, the term "apparent" alerts the reader to the fact that casual application of Gibbs' adsorption isotherm using C_B instead of activity treats solutes (proteins and surfactants) as isomerically-pure, non-ionized polyelectrolytes[33] at infinite dilution with unit activity coefficients.[34] Table 3 collects results for proteins studied in this work. The average Γ_{lv} = 179 $\pm$ 27 picomoles/cm^2 previously reported to be characteristic of the proteins listed in Table 1[4] was used in calculation of $\left[\Gamma_{\mathrm{sl}} - \Gamma_{sv}\right]$ and $\left\{\dfrac{\left[\Gamma_{\mathrm{sl}} - \Gamma_{sv}\right]}{\Gamma_{lv}}\right\}$.

Fig. 5A shows the MW dependence of apparent $\left[\Gamma_{\mathrm{sl}} - \Gamma_{sv}\right]$ adsorbing to the PS surface and compares these results to Γ_{lv} (Panel B; data from ref. 4) for these proteins adsorbing to the

buffer-air surface, as well as the ratio $\left\{\frac{\left[\Gamma_{\mathrm{sl}}-\Gamma_{sv}\right]}{\Gamma_{lv}}\right\}$ (Panel C). Fig. 6 plots $\left[\Gamma_{\mathrm{sl}}-\Gamma_{sv}\right]$ (Panel A) and $\left\{\frac{\left[\Gamma_{\mathrm{sl}}-\Gamma_{sv}\right]}{\Gamma_{lv}}\right\}$ (Panel B) as a function of surface wettability; where the buffer-air surface is assigned an adhesion tension equal to -73 mN/m corresponding to a hypothetical contact angle of 180^{o} that would be characteristic of a completely non-wetting surface. Note that $\left[\Gamma_{\mathrm{sl}}-\Gamma_{sv}\right]=-\Gamma_{lv}$ for the fully-wetted SiO_x surface, which is the $\theta_a \to 0^o$ limit on Eq. (1).[10, 11]

5.0 Discussion

Adsorption Reversibility: One of the more contentious issues in the protein-adsorption literature is reversibility of the protein-adsorption process. As a consequence, applicability of thermodynamic models such as Gibbs' surface excess to tensiometric data is frequently called into question. Needless to say perhaps, achievement of true thermodynamic equilibrium under experimental conditions such as those applied herein is not realistically possible because the semi-closed tensiometer chamber inevitably allows slow evaporation of small droplets and is relatively crudely thermostated; to say nothing of slow surface hydration effects discussed in the preceding section. Indeed, the experimentally observed steady-state achieved or asymptotically approached within 1 hour drop age in tensiometric experiments has been referred to as a "pseudo" or "meso" equilibrium,[10, 11] in recognition of longer-term protein-denaturation effects that can include loss of higher-order structure and commensurate changes in molar volume (see ref. 37 and citations therein) that can slowly affect measured interfacial tensions. Thus, true thermodynamic equilibrium is a forgone conclusion. Rather, the practical issue at hand is whether protein adsorption observed herein achieves a steady-state that is due to a substantially reversible process that can be meaningfully modeled using propositions based on thermodynamic ideality.

Although adsorption reversibility is technically challenging to prove, it turns out that irreversible adsorption is quite straightforward to *unambiguously disprove* for those circumstances in which this may occur, thereby eliminating irreversible adsorption as an argument that can be sensibly made against application of thermodynamics as an analysis tool. We have shown that protein adsorption to many surface types is not inherently irreversible using the standard solution-depletion method of measuring adsorption supplemented with protein-adsorption competition studies.[13-16] The basic idea behind the depletion method is to measure the concentration of protein *i* in solution before and after contact with test particulate adsorbents. The depletion method is thus substantially free of experimental artifacts; such as solute labeling, rinsing/drying, or complicated instrumentation. Using the depletion method under similar experimental conditions applied in tensiometric studies discussed herein (adsorption from stagnant fluids), we have shown that adsorption isotherms are linear with protein-solution concentration, consistent with a simple Henry isotherm, with fractional slope up to surface saturation.[13, 14, 16] Fractional slope means that protein distributes between solution and surface region in a manner consistent with reversible adsorption controlled by a modest partition coefficient P_i over a broad concentration range. Otherwise, if protein adsorbed irreversibly or with very high avidity (*i.e.* $P_i \to \infty$), then the adsorbent would completely-or-substantially deplete the solution of protein, leading to unitary slopes because the measured solution depletion would equal the initial solution concentration. This not being the case for a wide variety of proteins adsorbing to surfaces spanning the full range of water wettability, including ion-exchange surfaces,[16] we conclude that protein adsorption is not an inherently irreversible process. Specifically, we mean by this that although protein may irreversibly adsorb to some surfaces under certain experimental conditions, we do not observe irreversible protein adsorption to the surfaces studied herein under experimental conditions applied. Furthermore, using protein adsorption competition as a probe of irreversible adsorption, we have demonstrated that protein

i can displace protein *j* adsorbed to a broad range of surfaces.[5, 15, 16] Displacement of protein *i* by protein *j* is not possible if protein *i* is irreversibly adsorbed, corroborating our conclusion that protein adsorption is not an inherently irreversible process.

More inferential lines of evidence supporting reversible adsorption include:[7]

1. Concentration-dependent γ_{lv} and θ_a of proteins spanning 3 decades in MW (referred to as 'protein' or 'proteins' below) were like those obtained with small-molecule surfactants in that both followed expectations of Gibbs' adsorption isotherm[10, 11] with a linear-like decrease in γ_{lv} and θ_a as a function of concentration expressed on a logarithmic concentration axis.
2. Surface excess values (Γ_{lv} and $\left[\Gamma_{sl} - \Gamma_{sv}\right]$) computed from Gibbs' isotherm for surfactant standards agreed with independent instrumental methods of analysis within experimental error and surface excess values for proteins adsorbed to buffer-air and methyl-terminated SAM surfaces were statistically identical.[7]
3. Concentration-dependant γ_{lv} and θ_a continuously decreased as a function of protein solution concentration, well past the concentration required to fill the surface at theoretical monolayer coverage anticipated for irreversible adsorption.[3-5, 7-9]
4. Proteins were observed to be weak surfactants[1, 38] consistent with weakly adsorbed compounds with a commensurately low partition coefficient deduced from concentration-dependent γ_{lv} measurements.[4] Free energy of protein adsorption to hydrophobic surfaces calculated from these partition coefficients were in good agreement with values measured by hydrophobic interaction chromatography.[13, 39]
5. Protein adsorption to hydrophobic surfaces followed a 'Traube-like' ordering wherein the molar concentration required to achieve an arbitrary spreading pressure decreased in regular progression with MW.

6. Competitive-protein adsorption experiments at hydrophobic surfaces demonstrate protein displacement that follows a mass-balance exchange predicated on reversible adsorption.[5, 15]

These overlapping and independent lines of evidence[40-44] (see also ref. 38 for a review) supports application of Gibbsian surface thermodynamics as a reasonable model to quantify concentration-dependent interfacial tensions and contact angles as long as the non-ideal behavior of polyelectrolyte adsorbents is borne in mind in the interpretation of surface excess values.

Apparent Gibbs' Surface Excess: Fig. 5 compares the MW dependence of apparent $\left[\Gamma_{sl} - \Gamma_{sv}\right]$ (Panel A) for proteins of Table 1 adsorbing to the PS surface to Γ_{lv} (Panel B; data from ref. 4) and the ratio $\left\{\frac{\left[\Gamma_{sl} - \Gamma_{sv}\right]}{\Gamma_{lv}}\right\}$ (Panel C). It is evident from this data that the profound biochemical diversity among the broad range of proteins selected for study spanning nearly 3 decades in MW had little measurable effect on the interfacial energetics that controls the amount adsorbed to PS or LV surfaces from aqueous buffer solution.[3, 8] Adsorption to PS was similar to the methyl-terminated SAM surface in this regard.[7] However, the average $\left[\Gamma_{sl} - \Gamma_{sv}\right]$ for the PS surface was about 40% less than either the LV or CH_3 SAM surface,[7] presumably because PS was more hydrophilic (less hydrophobic) which commensurately reduced the overall driving force for protein adsorption.

Fig. 6A examines the relationship between protein adsorption and surface wettability in greater detail by plotting the mean $\left[\Gamma_{sl} - \Gamma_{sv}\right]$ value for all proteins studied at each surface as a function of water adhesion tension for CH_3 SAM, PS, APTES, and fully water-wettable SiO_x surfaces (see annotations for surface identity; error bars are the standard deviation of the mean; see

Table 3). Fig. 6B includes the LV case by plotting the ratio $\left\{\frac{\left[\Gamma_{sl}-\Gamma_{sv}\right]}{\Gamma_{lv}}\right\}$; where the ratio is unity by definition for the LV case. It is evident from Fig. 6 that surface excess generally decreased with surface wettability, passing through $\left[\Gamma_{sl}-\Gamma_{sv}\right]=0$ (no protein adsorbed if $\Gamma_{sv}\sim 0$) near a projected surface wettability $\tau^o \sim 30$ mN/m ($\theta_a = 65^o$). This result is consistent with the conclusion drawn from independent studies[12, 14] that water is too strongly bound to surfaces with $\tau^o \geq 30$ mN/m ($\theta_a \leq 65^o$) to be displaced by adsorbing protein and that, as a consequence, protein does not accumulate within the interfacial region at concentrations exceeding that of bulk solution.[38, 45, 46] It is further evident that $\left[\Gamma_{sl}-\Gamma_{sv}\right]<0$ for surfaces with $\tau^o > 30$ mN/m ($\theta_a < 65^o$). Our interpretation is that Γ_{sv} exceeds Γ_{sl} on progressively hydrophilic surfaces because protein deposits at the SV interface by evaporation as drops spread thinly on hydrophilic surfaces. This process culminates with $\Gamma_{sv}\rightarrow\Gamma_{lv}$ as $\tau^o \rightarrow 72$ mN/m ($\theta_a \rightarrow 0^o$), consistent with theoretical boundary conditions on Eq. (1).[10, 11] In general, the shape of the curve drawn through the data of Fig. 6A,B is consistent with these boundary conditions on Eq. (1), passing from maximal adsorption at the most hydrophobic LV surface, through decreasing adsorption on increasingly hydrophilic surfaces (methyl-terminated SAM and PS), to no measurable adsorption for $\tau^o \geq 30$ mN/m surfaces. The “adsorption mapping method” is a much less labor intensive approach to monitoring adsorption as a function of surface energy that leads to similar conclusions from data gathered using surfaces with incrementally-varied wetting properties.[12]

Conclusions:

Concentration-dependent contact angles can be used to monitor protein adsorption from aqueous-buffer solution to surfaces spanning the full range of water wetting characteristics. Adsorption trends can be quantified from contact angles by the apparent Gibbs' surface excess parameter using as-prepared molar solution concentrations as a measure of solute chemical potential. However, estimation of absolute Gibbs' excess quantities requires correction of apparent values by a factor of approximately 60 to account for the non-ideal chemical activity of proteins. Apparent Gibbs' surface excess varies by less than 25% for a broad range of blood proteins spanning 3 decades in molecular weight adsorbing to any particular surface. This level of protein-to-protein variation cannot be confidently distinguished from experimental error in apparent surface excess. Apparently, the biochemical diversity among proteins studied has little-or-no effect on the interfacial energetics that drives protein adsorption from aqueous solution.[3, 4, 6-9] Experiment shows that protein adsorption is not inherently irreversible and a variety of evidence supports application of surface thermodynamics as modeling tool to help understand energy balance in protein adsorption.

Protein adsorption as measured by Gibbs' excess decreases with increasing surface hydrophilicity to immeasurably-small values for surfaces exhibiting $\tau^o \geq 30$ mN/m ($\theta_a \leq 65^o$). These latter results corroborate the conclusion drawn from independent studies that water is too strongly bound to surfaces with $\tau^o \geq 30$ mN/m to be displaced by adsorbing protein and that, as a consequence, protein does not accumulate within the interfacial region of such surfaces at concentrations exceeding that of bulk solution ($\left[\Gamma_{sl} - \Gamma_{sv}\right] = 0$ at $\tau^o = 30$ mN/m). Thus it appears that water controls protein adsorption to surfaces and that the mechanism of protein adsorption can be understood from this perspective for a diverse set of proteins with very different amino-acid composition.[14]

Acknowledgements: This work was supported, in part, by from the National Institute of Health PHS 2R01HL069965 and the American Chemical Society Petroleum Research Fund grant #44523-AC5. Authors appreciate additional support from the Materials Research Institute and Departments of Bioengineering and Materials Science and Engineering, Penn State University. The authors appreciate the gracious assistance Mr. Nick Dellas and Professor Evangelos Manias with profilometry and atomic force microscopy.

Citations

1. Vogler, E. A., Interfacial Chemistry in Biomaterials Science. In *Wettability*, Berg, J., Ed. Marcel Dekker: New York, 1993; Vol. 49, pp 184-250.

2. Yaminsky, V. V.; Vogler, E. A., Hydrophobic Hydration. *Current Opinion in Colloid and Interface Sci.* **2001,** 6, 342-349.

3. Krishnan, A.; Sturgeon, J.; Siedlecki, C. A.; Vogler, E. A., Scaled Interfacial Activity of Proteins at the Liquid-Vapor Interface. *J. Biomed. Mat. Res.* **2004,** 68A, 544-557.

4. Krishnan, A.; Siedlecki, C.; Vogler, E. A., Traube-Rule Interpretation of Protein Adsorption to the Liquid-Vapor Interface. *Langmuir* **2003,** 19, 10342-10352.

5. Krishnan, A.; Siedlecki, C. A.; Vogler, E. A., Mixology of Protein Solutions and the Vroman Effect. *Langmuir* **2004,** 20, (12), 5071-5078.

6. Krishnan, A.; Wilson, A.; Sturgeon, J.; Siedlecki, C. A.; Vogler, E. A., Liquid-Vapor Interfacial Tension of Blood Plasma, Serum and Purified Protein Constituents Thereof. *Biomaterials* **2005,** 26, 3445-3453.

7. Krishnan, A.; Liu, Y.-H.; Cha, P.; Allara, D. L.; Vogler, E. A., Interfacial Energetics of Globular-Blood Protein Adsorption to a Hydrophobic Surface from Aqueous-Buffer Solution. *Journal of the Royal Society Interface* **2006,** 3, 283-301.

8. Krishnan, A.; Liu, Y.-H.; Cha, P.; Allara, D. L.; Vogler, E. A., Scaled Interfacial Activity of Proteins at a Hydrophobic Solid/Aqueous-Buffer Interface. *J. Biomed. Mater. Res.* **2005,** 75A, (2), 445-457.

9. Krishnan, A.; Liu, Y.-H.; Cha, P.; Allara, D. L.; Vogler, E. A., Interfacial Energetics of Blood Plasma and Serum Adsorption to a Hydrophobic Self-Assembled Monolayer Surface. *Biomaterials* **2006,** 27, 3187-3194.

10. Vogler, E. A., Practical Use of Concentration-Dependent Contact Angles as a Measure of Solid-Liquid Adsorption I: Theoretical Aspects. *Langmuir* **1992,** 8, 2005-2012.

11. Vogler, E. A., Practical Use of Concentration-Dependent Contact Angles as a Measure of Solid-Liquid Adsorption II: Experimental Aspects. *Langmuir* **1992, 8**, 2013-2020.

12. Vogler, E. A.; Martin, D. A.; Montgomery, D. B.; Graper, J. C.; Sugg, H. W., A Graphical Method for Predicting Protein and Surfactant Adsorption Properties. *Langmuir* **1993, 9**, 497-507.

13. Noh, H.; Vogler, E. A., Volumetric Interpretation of Protein Adsorption: Partition Coefficients, Interphase Volumes, and Free Energies of Adsorption to Hydrophobic Surfaces. *Biomaterials* **2006,** 27, 5780-5793.

14. Noh, H.; Vogler, E. A., Volumetric Interpretation of Protein Adsorption: Mass and Energy Balance for Albumin Adsorption to Particulate Adsorbents with Incrementally-Increasing Hydrophilicity. *Biomaterials* **2006,** 27, 5801-5812.

15. Noh, H.; Vogler, E. A., Volumetric Interpretation of Protein Adsorption: Competition from Mixtures and the Vroman Effect. *Biomaterials* **2007,** 28, 405-422.

16. Noh, H.; Vogler, E. A., Volumetric Interpretation of Protein Adsorption: Ion-Exchange Adsorbent Capacity, Protein pI, and Interaction Energetics. *Biomaterials* **2006,** in review.

17. Putnam, F. W., Alpha, Beta, Gamma, Omega - The Roster of the Plasma Proteins. In *The Plasma Proteins: Structure, Function, and Genetic Control*, Putnam, F. W., Ed. Academic Press: New York, 1975; Vol. 1, pp 58-131.

18. Anderson, N. L.; Anderson, N. G., The Human Plasma Proteome: History, Character, and Diagnostic Prospects. *Molecular and Cellular Proteomics* **2002,** 1, (11), 845-867.

19. Porter, M. D.; Bright, T. B.; Allara, D. L.; Chidseyi, C. E. D., Spontaneously Organized Molecular Assemblies. 4. Structural Characterization of n-Alkyl Thiol Monolayers on Gold by Optical Ellipsometry, Infrared Spectroscopy, and Electrochemistry. *J. Am. Chem. Soc* **1987,** 109, 3559-3568.

20. Nuzzo, R. G.; Dubois, L. H.; Allara, D. L., Fundamental Studies of Microscopic Wetting on Organic Surfaces 1. Formation and Structural Characterization of a Self Consistent Series of Polyfunctional Organic Monolayers. *J. Am. Chem. Soc.* **1990,** 112, (2), 558-569.

21. Nuzzo, R. G.; Allara, D. L., Adsorption of bifunctional organic disulfides on gold surfaces. *J. Am. Chem. Soc.* **1983,** 105, (13), 4481.

22. Nuzzo, R. G.; Fusco, F.; Allara, D. L., Spontaneously organized molecular assemblies. 3. Preparation and properties of solution adsorbed monolayers of organic disulfides on gold surfaces. *J. Am. Chem. Soc.* **1987,** 109, (8), 2358.

23. Nuzzo, R. G.; Dubois, L. H.; Allara, D. L., Fundamental studies of microscopic wetting on organic surfaces. 1. Formation and structural characterization of a self-consistent series of polyfunctional organic monolayers. *J. Am. Chem. Soc.* **1990,** 112, (2), 558.

24. Allara, D. L.; Nuzzo, R. G., Spontaneously Organized Molecular Assemblies. 2. Quantitative Infrared Spectroscopic Determination of
Equilibrium Structures of Solution-Adsorbed n -Alkanoic Acids on an Oxidized Aluminum Surface. *Langmuir* **1985,** Vol. 1, (1), 52-66.

25. Nuzzo, R. G.; Fusco, F. A.; Allara, D. L., Spontaneously Organized Molecular Assemblies. 3. Preparation and Properties of Solution Adsorbed Monolayers of Organic Disulfides on Gold Surfaces. *J. Am. Chem. Soc.* **1987,** 109, 2358-2368.

26. Bancroft, W. B., Breath Figures. *Phil. Mag.* **1892,** 24, (5), 180-196.

27. Lee, Y.-L.; Chou, W.-S.; Chen, L.-H., The Adsorption and Nucleation of Water Vapor on an Insoluble Spherical Solid Particle. *Surface Science* **1998,** 414, 363-373.

28. Frank, B.; Garoff, S., Temporal and Spatial Development of Surfactant Self Assemblies Controlling Spreading of Surfactant Solutions. *Langmuir* **1995,** 11, 4333-4340.

29. Stange, T. G.; Mathew, R.; Evans, D. F., Scanning Tunneling Microscopy and Atomic Force Microscopy Characterization of Polystyrene Spin-Coated onto Silicon Surfaces. *Langmuir* **1992,** 8, 920-926.

30. Krishnan, A.; Liu, Y.-H.; Cha, P.; Allara, D. L.; Vogler, E. A., An Evaluation of Goniometric Methods. *J. Colloid and Interf. Sci.* **2005,** 43, 95-98.

31. Tripp, B. C.; Magda, J. J.; Andrade, J. D., Adsorption of Globular Proteins at the Air/Water Interface as Measured via Dynamic Surface Tension: Concentration Dependence, Mass-transfer Considerations, and Adsorption Kinetics. *J. Colloid and Interface Sci.* **1995,** 173, 16-27.

32. Rosen, M. J., *Surfactants and Interfacial Phenomena*. Wiley: New York, 1978; p xiv, 304.

33. Frommer, M. A.; Miller, I. R., Adsorption of DNA at the Air-Water Interface. *J. Phys. Chem.* **1968,** 72, (8), 2862-2866.

34. Strey, R.; Vilsanen, Y.; Aratono, M.; Kratohvil, J. P.; Yin, Q.; Friberg, S. E., On the Necessity of Using Activities in the Gibbs Equation. *J. Phys. Chem. B.* **1999,** 103, (43), 9112-9116.

35. Ariola, F.; Krishnan, A.; Vogler, E. A., Interfacial Rheology of Blood Proteins Adsorbed to the Aqueous-Buffer/Air Interface. *Biomaterials* **2006,** 27, 3404-3412.

36. Ratner, B. D.; Rosen, J. J.; Hoffman, A. S.; Scharpen, L. R., An ESCA Study of Surface Contaminants on Glass Substrates for Cell Adhesion. *Proc. Int. Symp. Contam. Control* **1978,** 4, 669-686.

37. Birdi, K. S., *Lipid and biopolymer monolayers at liquid interfaces*. Plenum Press: New York, 1989; p x, 325.

38. Vogler, E. A., Structure and Reactivity of Water at Biomaterial Surfaces. *Adv. Colloid and Interface Sci.* **1998,** 74, (1-3), 69-117.

39. Wen-Yih Chen, H.-M. H., Chien-Chen Lin, Fu-Yung Lin, and Yu-Chia Chan, Effect of Temperature on Hydrophobic Interaction between Proteins and Hydrophobic Adsorbents: Studies by Isothermal Titration Calorimetry and the van't Hoff Equation. *Langmuir* **2003,** 19, (22), 9395-9403.

40. Kamyshny, A.; Lagerge, S.; Partyka, S.; Relkin, P.; Magdassi, S., Adsorption of Native and Hydrophobized Human IgG onto Silica: Isotherms, Calorimetry, and Biological Activity. *Langmuir* **2001,** 17, (26), 8242 -8248.

41. Brash, J. L., Protein Adsorption at the Solid-Solution Interface in Relation to Blood-Material Interactions. In *ACS Symposium Series*, American Chemical Society: Washington D. C., 1987; Vol. 343, pp 490-506.

42. Duinhoven, S.; Poort, R.; Voet, G. V. d.; Agterof, W.; Norde, W.; Lyklema, J., Driving Forces for Enzyme Adsorption at Solid-Liquid Interfaces. 1. The Serine Protease Savinase. *J. Colloid and Interface Sci.* **1995,** 170, 340-350.

43. Graham, D. E.; Phillips, M. C., Proteins at Liquid Interfaces. *J. Colloid and Interface Sci.* **1979,** 70, (3), 415-426.

44. Castillo, E.; Koenig, J.; Anderson, J., Protein Adsorption on Hydrogels II. Reversible and Irreversible Interactions Between Lysozyme and Soft Contact Lens Surfaces. *Biomaterials* **1985,** 6, 338-345.

45. Vogler, E. A., Water and the Acute Biological Response to Surfaces. *J. Biomat. Sci. Polym. Edn.* **1999,** 10, (10), 1015-1045.

46. Vogler, E. A., How Water Wets Biomaterials. In *Water in Biomaterials Surface Science*, Morra, M., Ed. John Wiley and Sons: New York, 2001; pp 269-290.

List of Figure Legends

Figure 1: Advancing contact angle isotherms in 3D (θ_a as a function of observation time and logarithmic solution concentration $\ln C_B$ expressed in picomolar pM) and 2D (θ_a as a function of $\ln C_B$ at selected observation times) formats. Panels A-C compare thrombin (blood factor IIa) adsorption onto 1-hexadecanethiol self-assembled monolayer (SAM, Panel A), spun-coated polystyrene (PS, Panel B), and aminopropyltriethoxylsilane (APTES, Panel C) surfaces. Symbols in 2D panels represent time slices through 3D representations (filled circle = 90 s, open circle = 900 s, open triangles = 1800 s, and open squares = 3594 s). Annotations in Panel A indicate pure-buffer advancing contact angle θ_a^o and surface-saturated contact angle $\theta_a^{'}$ plateau values as well as maximum and half-maximum contact angle reductions, θ_a^{max} and $\frac{1}{2}\theta_a^{max}$, respectively, which occur at the characteristic solution concentration $\ln C_B^{\Theta/2}$. These contact angle parameters are collected in Table 2. Interfacial kinetics dominated adsorption of thrombin to SAM and PS surfaces but kinetics were not discernable in the APTES case. Notice that θ_a^o was observed to decrease with time for all surfaces due to a "hydration effect" that was especially evident for the APTES surface (see annotations in Panel C). Correction for the hydration effect revealed that protein adsorption achieved or asymptotically approached steady state for all proteins listed in Table 1.

Figure 2: Advancing contact angles θ_a^o for pure phosphate-buffered saline solution (PBS, left axis, closed circles) on spun-coated polystyrene (PS) decrease monotonically with observation-time due to a time-dependent "hydration" of the PS surface while liquid-vapor interfacial tension (γ_{lv}^o, right axis, open circles) remains constant. Test surface hydration also affects θ_a adsorption isotherms shown in Fig. 1 (arrow-annotation, Panel

C). Raw adsorption kinetics of human blood factor XII (FXII, 20 mg mL^{-1}) to PS (closed triangles) can be corrected for hydration effects (open triangles) by subtracting reduction observed in θ_a^o, revealing that adsorption comes to steady state within the 1 hour observation window.

Figure 3: Sequential interpretation of a steady-state (t=3600 s) contact angle isotherm for human serum albumin (FVHSA) adsorbing onto polystyrene (PS). Advancing contact angles (θ_a, Panel A) are converted into advancing adhesion tensions (τ_a, Panel B) and advancing spreading pressures (Π_a, Panel C). Smoothed curves through the data are guides to the eye. Annotations identify low- and high-concentration asymptotes for contact angles (θ_a° , $\theta_a^{'}$), adhesion tensions (τ_a° , $\tau_a^{'}$), respectively, and maximum spreading pressure (Π_a^{max}), used to characterize protein adsorption isotherms (Table 2).

Figure 4: Comparison of steady-state spreading pressure (Π_a) isotherms for selected proteins spanning three orders of magnitude in molecular weight (see Table 1) adsorbing to spun-coated polystyrene (PS). Smooth curves are guides to the eye. Molar concentration scaling reveals a “Traube-like rule” ordering among diverse proteins similar to that observed for proteins adsorbed to the buffer/air and buffer/SAM interfaces wherein molar concentration required to reach a specified Π_a value decreased with increasing MW (see arrow annotation).

Figure 5: Apparent Gibbs' surface excess for various proteins adsorbed to spun-coated polystyrene (PS) and buffer/air surface scaled by protein molecular weight MW (error bars represent estimated 1σ confidence intervals derived from propagation of experimental error into theoretical parameters). Gibbs' surface excess parameters $\left[\Gamma_{sl} - \Gamma_{sv}\right]$ (Panel A, PS) and Γ_{lv} (Panel B, buffer/air) reveal little statistically-discernable differences in the amount adsorbed to these surfaces among very different proteins spanning three-orders of magnitude in MW. Panel C plots data as the ratio $\left\{\frac{\left[\Gamma_{sl} - \Gamma_{sv}\right]}{\Gamma_{lv}}\right\}$ suggesting that approximately 65% less protein adsorbs to the PS surface than the buffer/air surface (see Fig. 6).

Figure 6: Apparent Gibbs' surface excess scaled as a function of adsorbent surface water wettability (surface energy) as measured by PBS advancing adhesion tension τ_a° for proteins and surfaces used in this study (see annotations for surface type; error bars represent mean and standard deviation for all proteins listed in Tables 1 and 2). Panel A shows that Gibbs' surface excess parameter $\left[\Gamma_{sl} - \Gamma_{sv}\right]$ decreases monotonically with increasing adsorbent-surface hydrophilicity, projecting $\left[\Gamma_{sl} - \Gamma_{sv}\right] = 0$ near $\tau_a^\circ = 30$ mN/m. Likewise, the ratio $\left\{\frac{\left[\Gamma_{sl} - \Gamma_{sv}\right]}{\Gamma_{lv}}\right\}$ decreases from +1 to -1 (Panel B) as $\left[\Gamma_{sl} - \Gamma_{sv}\right]$ decreases from a maximum $\left[\Gamma_{sl} - \Gamma_{sv}\right] = \Gamma_{lv}$ at the hydrophobic SAM surface ($\tau_a^\circ = -15$ mN/m) to a minimum $\left[\Gamma_{sl} - \Gamma_{sv}\right] = -\Gamma_{lv}$ at the water-wetted ($\tau_a^\circ = 73$ mN/m surfaces. Smoothed curves drawn through the data are guides to the eye.

Table 1. Purified Proteins.					
name of protein (abbreviation)	**molecular weight (kDa)**	**as-received form (mg/mL)**	**purity/ biologic activity**	**physiologic concentration (mg/100mL) [nominal value]**	**vendor**
human ubiquitin (Ub)	10.7	powder	98%	10-20 [15]	Sigma-Aldrich
human thrombin (FIIa)	35.6	powder	1411 NIH units/mg	n/a	Sigma-Aldrich
human serum albumin [fraction five] (FVHSA)	66.3	powder	98%	3500-5500 [4500]	Sigma-Aldrich
human prothrombin (FII)	72	powder	97%	5-10 [7.5]	Enzyme Research Labs.
human factor XII (FXII)	78	solution (2.1)	95%	[4]	Hematologic Technologies
human immunoglobin-G (IgG)	160	powder	97%	800-1800 [1300]	Sigma-Aldrich
human fibrinogen (Fb)	340	powder	70% clottable protein	200-450 [325]	Sigma-Aldrich
human complement component C1q (C1q)	400	solution (1.1)	single band by immunoelectrophoresis	10-25 [17.5]	Sigma-Aldrich
human α_2-macroglobulin (α–mac)	725	powder	98%	150-350 [250]	Sigma-Aldrich
human immunoglobin-M (IgM)	1000	solution (1.7) solution (1.1)	single band by immunoelectrophoresis	60-250 [155]	MP Biomedicals

Table 2. Steady-State Protein Adsorption Parameters.

name of protein (abbreviation)	θ_a° (°)	$\theta_a^{'}$ (°)	$\ln C_B^{\Theta/2}$ (PPT [p***M***])	***M*** (dimensionless)	τ_a° (mN m^{-1})	$\tau_a^{'}$ (mN m^{-1})	Π_a^{max} (mN m^{-1})
spin-coated polystyrene (PS) surface							
human ubiquitin (Ub)[a]	85.0±0.3	63.3	21.5 [19.2]	—	6.3	12.9	6.6
human thrombin (FIIa)	85.1±0.3	65.2±1.3	19.0±0.3 [15.4±0.3]	-13.2±2.0	6.2±0.4	20.3±1.0	14.0±1.4
human serum albumin [fraction five] (FVHSA)	82.6±0.7	57.0±1.2	14.7±0.3 [10.6±0.3]	-8.4±1.4	9.2±0.9	25.3±0.8	16.1±1.6
human prothrombin (FII)	84.3±0.3	69.0±0.5	16.9±0.2 [12.6±0.2]	-21.8±4.0	7.0±0.4	15.8±0.4	8.8±0.7
human factor XII (FXII)	87.7±0.3	66.3±1.3	16.8±0.3 [12.5±0.3]	-12.7±2.1	2.8±0.4	14.6±0.7	11.8±1.1
human immunoglobin-G (IgG)	83.6±0.6	67.7±1.2	16.2±0.4 [11.1±0.4]	-11.1±2.8	8.0±0.7	19.5±1.0	11.5±1.7
human fibrinogen (Fb) **prep. 1**	83.1±0.3	65.9±0.4	16.3±0.1 [10.5±0.1]	-21.7±3.2	8.4±0.4	19.4±0.3	11.0±0.7
prep. 2	84.0±0.3	64.7±0.4	15.5±0.1 [9.7±0.1]	-19.5±2.3	7.4±0.4	20.4±0.8	13.0±1.2
human complement component C1q (C1q)	85.3±0.3	66.1±1.2	16.0±0.3 [10.0±0.3]	-10.7±1.5	5.9±0.3	22.0±1.0	16.1±1.4
human α$_2$-macroglobulin (α–mac)	82.5±0.3	67.1±0.5	16.9±0.2 [10.3±0.2]	-19.7±3.0	9.3±0.3	22.2±0.4	12.9±0.8
human immunoglobin-M (IgM)	82.8±0.4	63.4±0.9	14.4±0.2 [7.5±0.3]	-10.6±1.7	9.0±0.5	22.6±0.7	13.6±1.2
aminopropyltriethoxysilane-treated (APTES) surface							
human thrombin (FIIa)	49.5±0.2	52.7±0.4	14.9±0.2 [11.3±0.2]	54.8 ±34.3	43.8±0.2	31.3±0.3	-12.4±0.5
human serum albumin [fraction five] (FVHSA)	61.7±0.4	54.3±0.8	17.3±1.1 [13.1±1.1]	-28.7±0.8	27.1±0.5	33.6±0.4	6.6±0.9
human complement component C1q (C1q)	52.9±0.2	47.2±0.5	11.0±0.3 5.1±0.3	-5.6±0.8	37.0±0.4	43.2±0.2	6.4±0.6
human immunoglobin-M (IgM)	47.3±0.1	53.7±0.3	10.7±0.1 [3.8±0.1]	22.5±3.7	48.6±0.2	29.9±0.2	-18.6±0.4

[a]Parameters are graphical estimates of fitted parameters. (See Results section.)

Table 3. Gibbs' Surface Excess.				
name of protein (abbreviation)		**apparent surface excess[a] (picomoles/cm^2)**		
		$[\Gamma_{sl} - \Gamma_{sv}]$	Γ_{lv}	$\left\{\frac{[\Gamma_{sl} - \Gamma_{sv}]}{\Gamma_{lv}}\right\}$
spin-coated polystyrene (PS) surface				
human ubiquitin (Ub)[b]		148	179±27	0.8
human thrombin (FIIa)		68.5±23.4		0.4±0.2
human serum albumin [fraction five] (FVHSA)		77.7±29.3		0.4±0.3
human prothrombin (FII)		128±38		0.7±0.4
human factor XII (FXII)		123±29		0.7±0.3
human immunoglobin-G (IgG)		68.1±33.0		0.4±0.3
human fibrinogen (Fb)	**prep. 1**	184±41		1.0±0.5
	prep. 2	200±32		1.1±0.4
human complement component C1q (C1q)		89.8±21.9		0.5±0.2
human α_2-macroglobulin ($\bar{\alpha}$mac)		116±25		0.6±0.3
human immunoglobin-M (IgM)		100±29		0.6±0.3
aminopropyltriethoxysilane-treated (APTES) surface				
human thrombin (FIIa)		-214±61	179±27	-1.2±0.6
human serum albumin [fraction five] (FVHSA)		-4.2±46.8		-0.0±0.3
human complement component C1q (C1q)		90.0±1.1		0.5±0.1
human immunoglobin-M (IgM)		-222.±27		-1.2±0.1

[a]Apparent $[\Gamma_{sl} - \Gamma_{sv}]$ or Γ_{lv} is computed without activity correction. (See Discussion section).

[b]Parameters are graphical estimates of fitted parameters. (See Results section.)

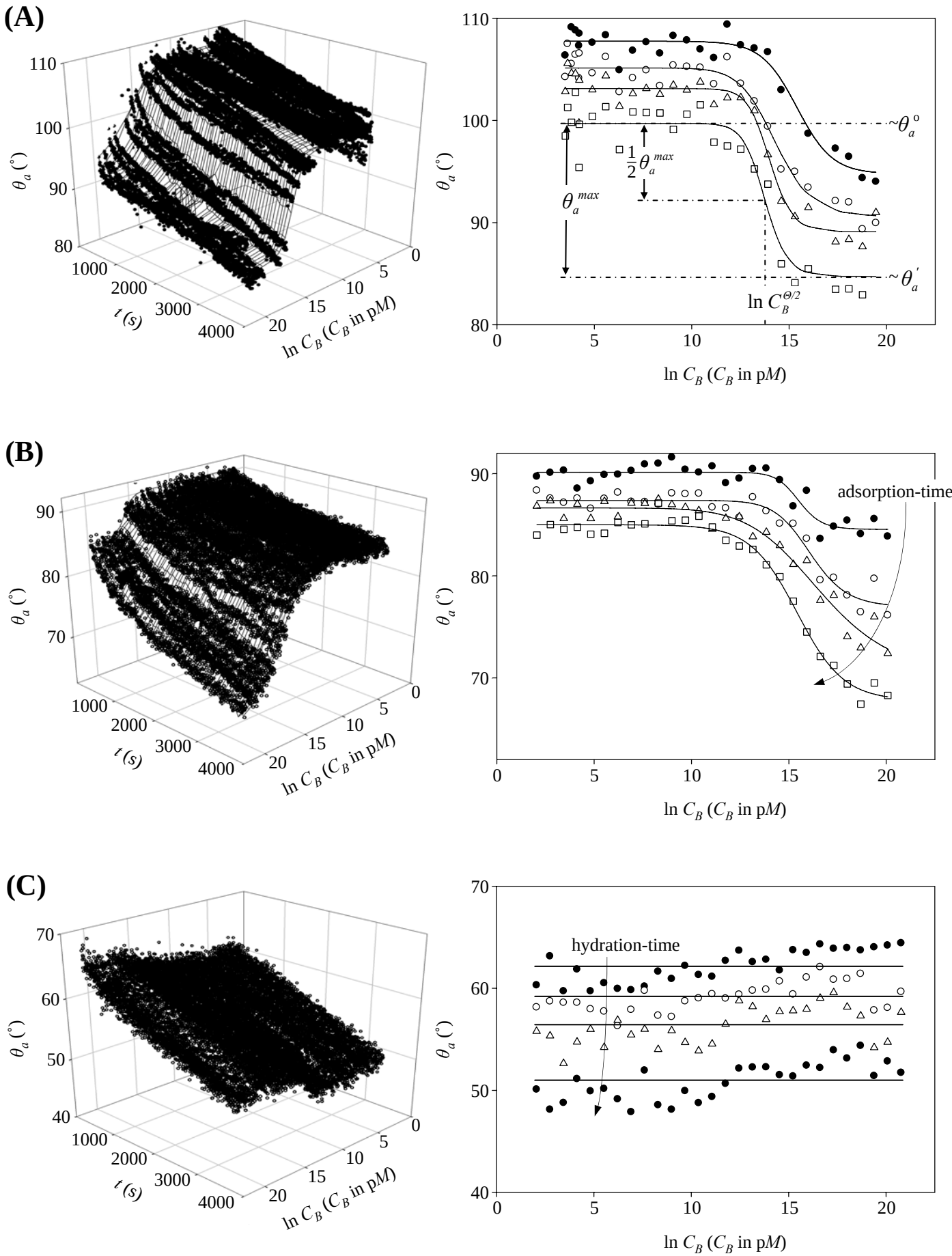
(A)
110
100
90
80
θ_a (°)
1000
2000
3000
4000
t (s)
0
5
10
15
20
ln C_B (C_B in pM)
110
100
90
80
θ_a (°)
$\sim\theta_a^{o}$
$\frac{1}{2}\theta_a^{max}$
θ_a^{max}
$\sim\theta_a'$
ln $C_B^{\theta/2}$
0
5
10
15
20
ln C_B (C_B in pM)
(B)
90
80
70
θ_a (°)
1000
2000
3000
4000
t (s)
0
5
10
15
20
ln C_B (C_B in pM)
90
80
70
θ_a (°)
adsorption-time
0
5
10
15
20
ln C_B (C_B in pM)
(C)
70
60
50
40
θ_a (°)
1000
2000
3000
4000
t (s)
0
5
10
15
20
ln C_B (C_B in pM)
70
60
50
40
θ_a (°)
hydration-time
0
5
10
15
20
ln C_B (C_B in pM)

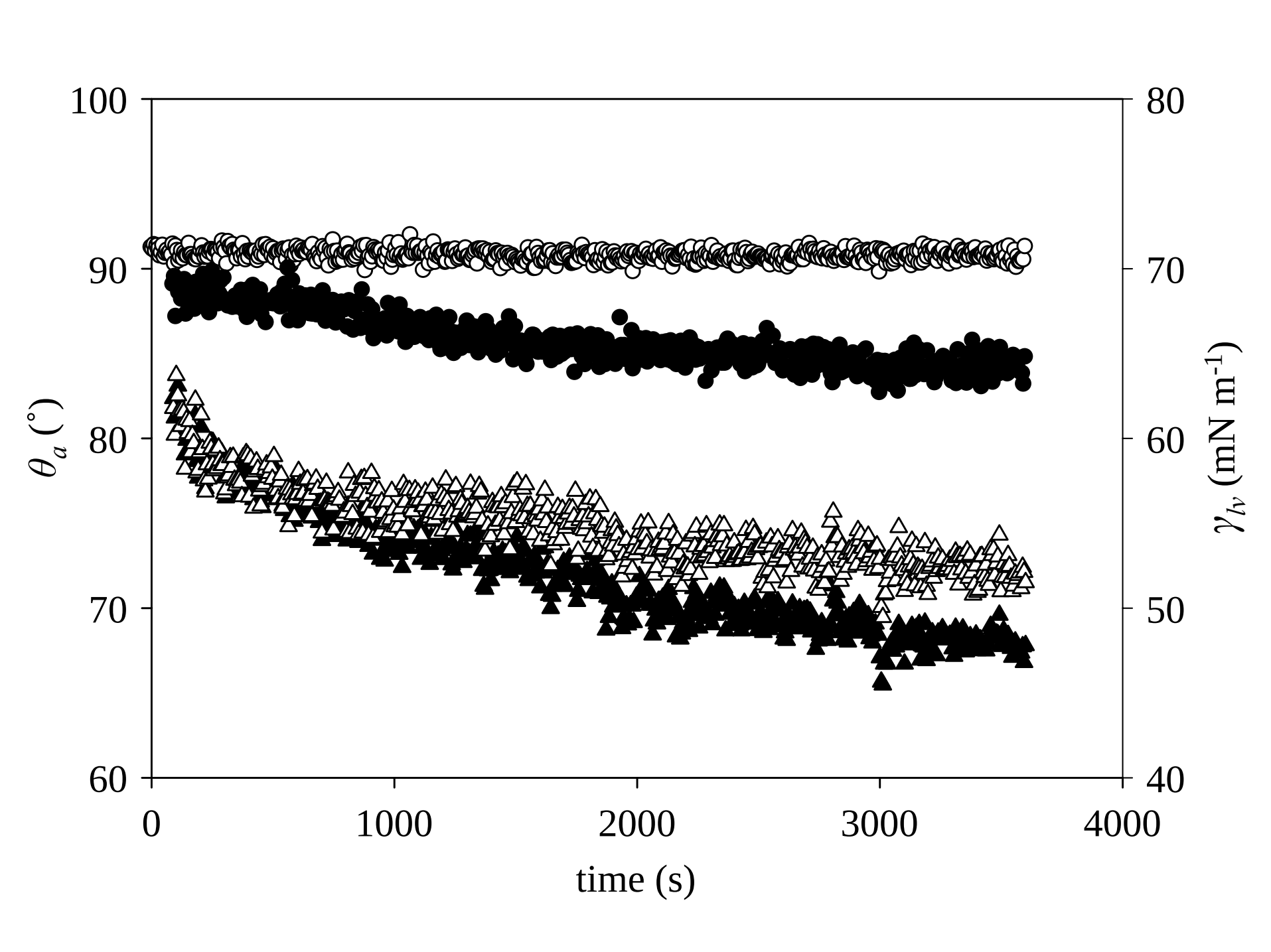
100
90
80
70
60
80
70
60
50
40
0
1000
2000
3000
4000
time (s)
θ_a (°)
γ_{lv} (mN m^{-1})

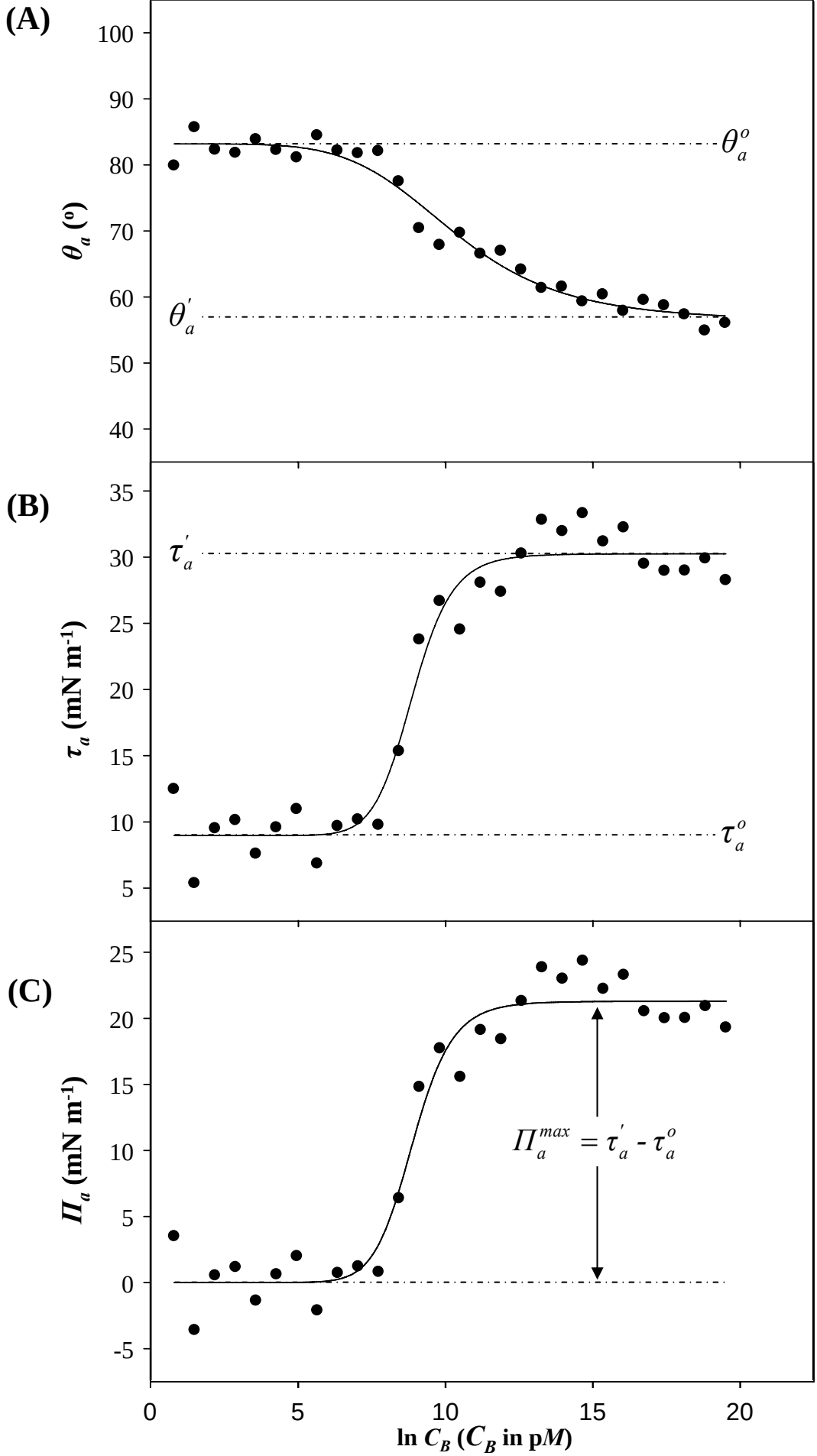
(A)
100
90
80
70
60
50
40
θ_a (°)
θ_a^o
θ_a'
(B)
35
30
25
20
15
10
5
τ_a (mN m^{-1})
τ_a'
τ_a^o
(C)
25
20
15
10
5
0
-5
Π_a (mN m^{-1})
$\Pi_a^{max} = \tau_a' - \tau_a^o$
0
5
10
15
20
ln C_B (C_B in pM)

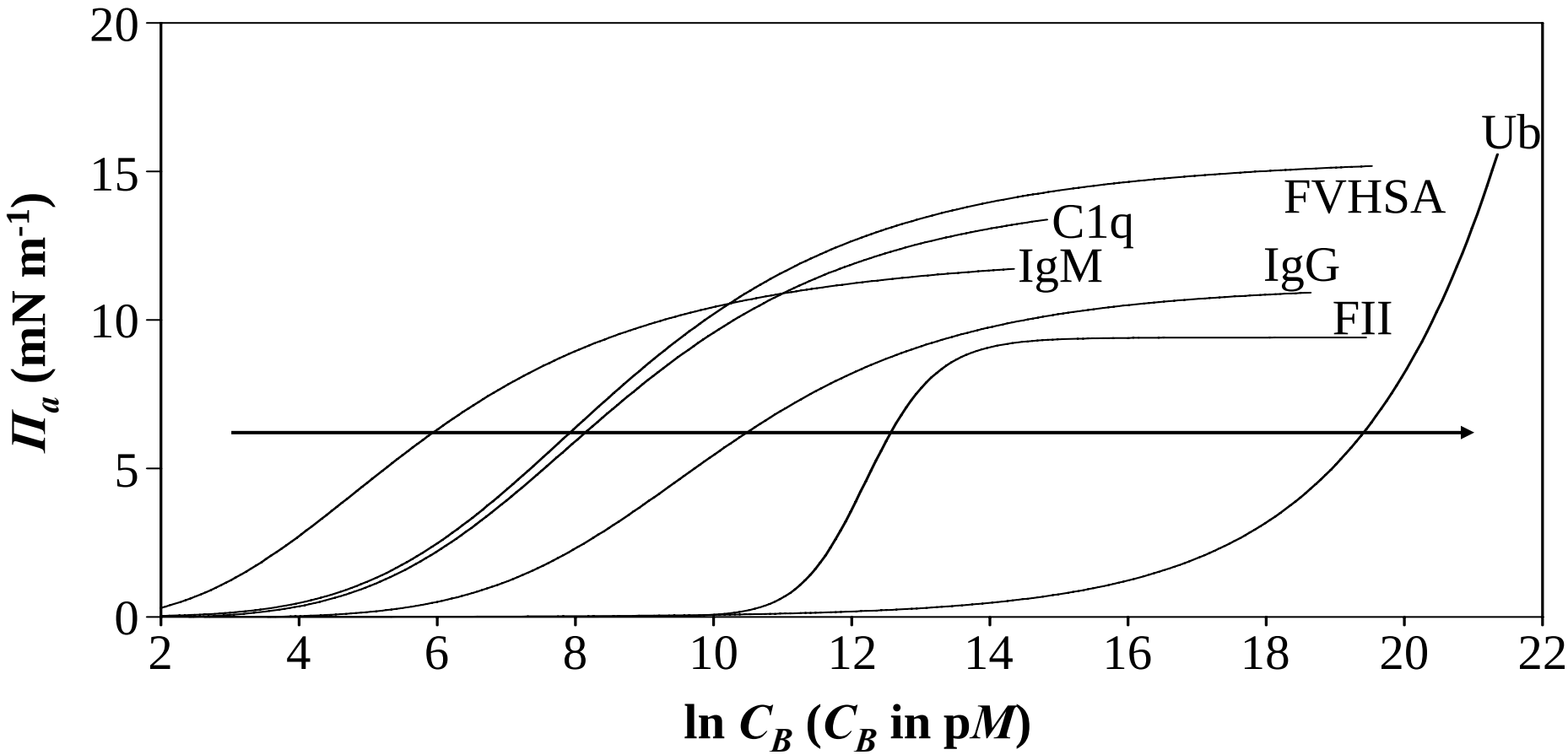
20
15
10
5
0
2
4
6
8
10
12
14
16
18
20
22
Ub
FVHSA
C1q
IgM
IgG
FII
Π_a (mN m^{-1})
ln C_B (C_B in pM)

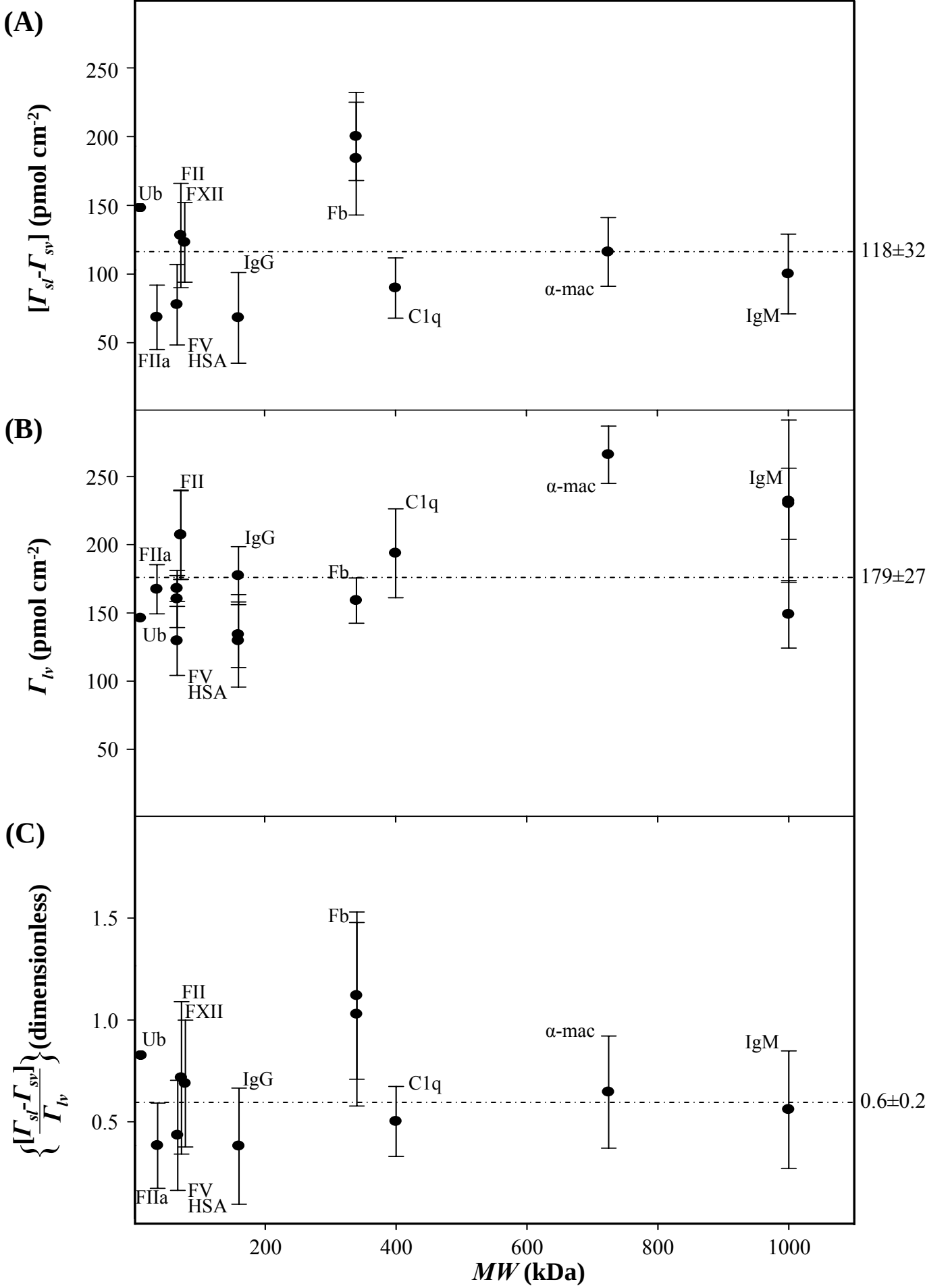
(A)
$[\Gamma_{sl}-\Gamma_{sv}]$ (pmol cm^{-2})
250
200
150
100
50
Ub
FII
FXII
Fb
IgG
C1q
α-mac
IgM
FIIa
FV
HSA
118±32
(B)
Γ_{lv} (pmol cm^{-2})
250
200
150
100
50
FII
FIIa
IgG
Fb
C1q
α-mac
IgM
Ub
FV
HSA
179±27
(C)
$\left\{\frac{[\Gamma_{sl}-\Gamma_{sv}]}{\Gamma_{lv}}\right\}$ (dimensionless)
1.5
1.0
0.5
Fb
FII
FXII
Ub
IgG
C1q
α-mac
IgM
FIIa
FV
HSA
0.6±0.2
200
400
600
800
1000
MW (kDa)

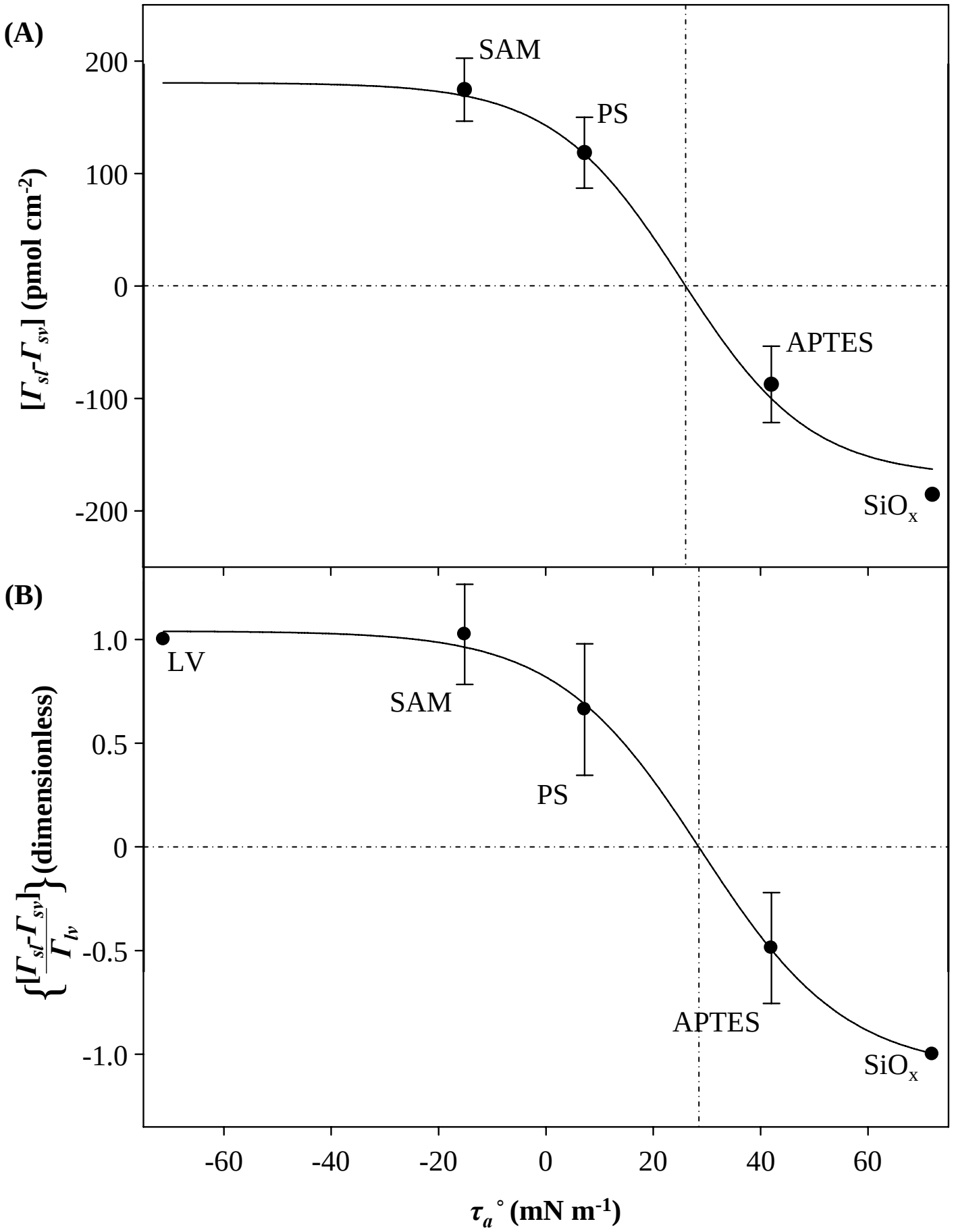
(A)
200
100
0
-100
-200
$[\Gamma_{sl}\text{-}\Gamma_{sv}]$ (pmol cm^{-2})
SAM
PS
APTES
SiO$_x$
(B)
1.0
0.5
0
-0.5
-1.0
$\left\{\frac{[\Gamma_{sl}\text{-}\Gamma_{sv}]}{\Gamma_{lv}}\right\}$(dimensionless)
LV
SAM
PS
APTES
SiO$_x$
-60
-40
-20
0
20
40
60
τ_a ° (mN m^{-1})

Table of Contents Graphic: